

A physicochemical framework for interpreting the biological calcification response to CO₂-induced ocean acidification

Justin B. Ries*

Department of Marine Sciences, University of North Carolina—Chapel Hill, 4202G Venable Hall, Campus Box 3300, Chapel Hill, NC 27599, USA

Department of Geology and Geophysics, Woods Hole Oceanographic Institution, Woods Hole, MA 02543, USA

Received 16 June 2010; accepted in revised form 22 April 2011; available online 1 May 2011

Abstract

A generalized physicochemical model of the response of marine organisms' calcifying fluids to CO₂-induced ocean acidification is proposed. The model is based upon the hypothesis that some marine calcifiers induce calcification by elevating pH, and thus Ω_A , of their calcifying fluid by removing protons (H⁺). The model is explored through two end-member scenarios: one in which a fixed number of H⁺ is removed from the calcifying fluid, regardless of atmospheric $p\text{CO}_2$, and another in which a fixed external–internal H⁺ ratio ($[\text{H}^+]_E/[\text{H}^+]_I$) is maintained. The model is able to generate the full range of calcification response patterns observed in prior ocean acidification experiments and is consistent with the assertion that organisms' calcification response to ocean acidification is more negative for marine calcifiers that exert weaker control over their calcifying fluid pH. The model is empirically evaluated for the temperate scleractinian coral *Astrangia poculata* with in situ pH microelectrode measurements of the coral's calcifying fluid under control and acidified conditions. These measurements reveal that (1) the pH of the coral's calcifying fluid is substantially elevated relative to its external seawater under both control and acidified conditions, (2) the coral's $[\text{H}^+]_E/[\text{H}^+]_I$ is approximately the same under control and acidified conditions, and (3) the coral removes fewer H⁺ from its calcifying fluid under acidified conditions than under control conditions. Thus, the carbonate system dynamics of *A. poculata*'s calcifying fluid appear to be most consistent with the fixed $[\text{H}^+]_E/[\text{H}^+]_I$ end-member scenario. Similar microelectrode experiments performed on additional taxa are required to assess the model's general applicability.

© 2011 Elsevier Ltd. All rights reserved.

1. INTRODUCTION

Recent experiments have revealed that marine calcifiers exhibit a broad spectrum of calcification responses to CO₂-induced ocean acidification, including negative, threshold-negative, neutral, threshold-positive, parabolic, and positive (e.g., Fabry et al., 2008; Iglesias-Rodriguez et al., 2008; Wood et al., 2008; Doney et al., 2009; Ries et al., 2009; Rodolfo-Metalpa et al., 2010; Fig. 1). There is growing evidence that one of the primary factors controlling the response of individual species to CO₂-induced ocean acidification is their control over carbonate chemistry at their site

of calcification (e.g., Cohen and Holcomb, 2009; Ries et al., 2009). Here, two general end-member scenarios of calcification site chemistry (fixed H⁺-removal vs. fixed external–internal H⁺ ratio) are presented and explored under four atmospheric $p\text{CO}_2$ scenarios: 400, 600, 900, and 2850 ppm. The applicability of these model scenarios to the calcifying fluid of the temperate coral *Astrangia poculata* was empirically assessed by measuring the pH of the coral's calcifying fluid with H⁺-sensitive microelectrodes under control (non-acidified) and acidified conditions.

2. BIOLOGICAL CONTROL OVER CALCIFICATION SITE CHEMISTRY

Many calcifying marine organisms, including scleractinian corals (Al-Horani et al., 2003; Cohen and

* Tel.: +1 919 962 0269; fax: +1 919 962 1254.

E-mail addresses: riesjustin@gmail.com, jries@unc.edu

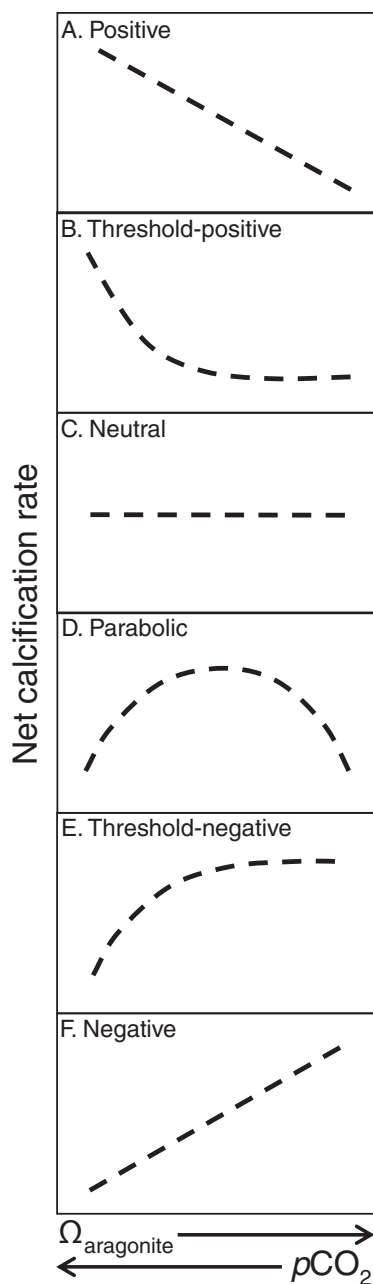


Fig. 1. Summary of the various biological calcification responses to CO_2 -induced ocean acidification (e.g., Langdon, 2000; Fabry et al., 2008; Iglesias-Rodríguez et al., 2008; Wood et al., 2008; Doney et al., 2009; Ries et al., 2009; Rodolfo-Metalpa et al., 2010): (A) positive; (B) threshold-positive; (C) neutral; (D) parabolic; (E) threshold-negative; (F) negative. Modified from Ries et al. (2009) and Ries (2010b).

McConnaughey, 2003; Cohen and Holcomb, 2009; Holcomb et al., 2009), coralline red algae (Borowitzka, 1987; McConnaughey and Whelan, 1997), calcareous green algae (Borowitzka, 1987; McConnaughey and Falk, 1991; De Beer and Larkum, 2001), foraminifera (Rink et al., 1998), and crabs (Cameron, 1985) are thought to facilitate precipitation of their skeletal or shell CaCO_3 by elevating pH at their site of calcification. The effect of pH on carbonate

chemistry at the site of calcification can be summarized by the following equilibrium reactions:



which are, respectively, governed by the following stoichiometric dissociation constants:

$$K^*_1 = [\text{HCO}_3^-][\text{H}^+]/[\text{H}_2\text{CO}_3] \quad \text{and} \quad (3)$$

$$K^*_2 = [\text{CO}_3^{2-}][\text{H}^+]/[\text{HCO}_3^-]. \quad (4)$$

Thus, reducing $[\text{H}^+]$ at the site of calcification shifts the carbonic acid system towards elevated $[\text{CO}_3^{2-}]$, thereby increasing CaCO_3 saturation state (Ω_{CaCO_3}):

$$\Omega_{\text{CaCO}_3} = [\text{Ca}^{2+}][\text{CO}_3^{2-}]/K^*_{\text{sp}}; \quad (5)$$

where K^*_{sp} is the stoichiometric solubility product of the appropriate CaCO_3 polymorph (e.g., calcite, aragonite, vaterite).

Various mechanisms have been proposed for elevating pH at the site of calcification, including conventional H^+ -channeling (McConnaughey and Falk, 1991), Ca^{2+} - H^+ exchanging ATPase (McConnaughey and Falk, 1991; McConnaughey and Whelan, 1997; Cohen and McConnaughey, 2003), light-induced H^+ -pumping (De Beer and Larkum, 2001), transcellular symporter and co-transporter H^+ -solute shuttling (McConnaughey and Whelan, 1997), cellular extrusion of hydroxyl ions (OH^-) into the calcifying medium, and CO_2 -consumption via photosynthesis (Borowitzka and Larkum, 1976).

The decrease in seawater pH that will accompany the forecasted rise in anthropogenic atmospheric $p\text{CO}_2$ will reduce seawater $[\text{CO}_3^{2-}]$, which has been shown to inhibit biological deposition of CaCO_3 , or even promote its dissolution (cf. Langdon, 2000; Kleypas et al., 2006; Fabry et al., 2008; Doney et al., 2009; Ries et al., 2009). However, if seawater is the source of an organism's calcifying fluid (e.g., Gaetani and Cohen, 2006), then the concentration of dissolved inorganic carbon (DIC) in this fluid will increase as atmospheric $p\text{CO}_2$ increases. Organisms able to maintain their calcifying fluid at sufficiently elevated pH, despite reduced external pH, will convert much of this increased DIC, occurring primarily as HCO_3^- , to CO_3^{2-} . Thus, when such organisms are exposed to elevated $p\text{CO}_2$, they may experience a $[\text{CO}_3^{2-}]$ in their calcifying fluid that is only slightly less than, or possibly equal to or greater than that attained under present-day atmospheric $p\text{CO}_2$ -depending upon the strength of their H^+ -regulating mechanism (Ries et al., 2009).

The removal of H^+ from an organism's calcifying fluid requires energy. Two factors that influence the amount of energy required to regulate calcification site pH are the quantity of H^+ removed from a given volume of the calcifying fluid and the H^+ -gradient across the membrane(s) that bounds the calcifying fluid (Goldman, 1943; Hodgkin and Katz, 1949; Kitasato, 1968; Saddler, 1970; Richards and Hope, 1974; McConnaughey and Falk, 1991). The energy required to maintain a H^+ -gradient across a membrane, known as the Nernst potential (E), is defined as:

$$E = \Delta G/(-nF); \quad (6)$$

where n is the valence charge of H^+ (1), F is the Faraday constant ($96485.3 \text{ C mol}^{-1}$), and ΔG is the Gibbs free energy of the system. The Gibbs free energy of the system can be defined as:

$$\Delta G = (-RT) \times \ln([H^+]_E/[H^+]_I) \quad (7)$$

where R is the universal gas constant ($8.31451 \text{ J K}^{-1} \text{ mol}^{-1}$), T is absolute temperature (298.16 at 25 °C), and $[H^+]_E$ and $[H^+]_I$ are H^+ concentrations of the external seawater and of the organism's calcifying fluid, respectively.

The Nernst potential (E) can therefore be defined as:

$$E = (RT)/(nF) \times \ln([H^+]_E/[H^+]_I) \quad (8)$$

Because R , T , n , and F are constants in the described H^+ -membrane system, the magnitude of the Nernst potential, or the energetic cost of maintaining a H^+ -gradient between external seawater and an organism's membrane-bound calcifying fluid, is proportional to the ratio of the external and internal H^+ concentrations ($[H^+]_E/[H^+]_I$).

3. MODELING CARBONATE SYSTEM CHEMISTRY AT THE SITE OF CALCIFICATION

To explore the effects of H^+ -pumping on the carbonate chemistry of calcifying fluids under various levels of atmospheric pCO_2 , two end-member scenarios of the calcifying fluid proton-pumping model are presented: one that assumes a fixed number of H^+ are removed from the calcifying fluid (i.e., variable $[H^+]_E/[H^+]_I$) under each atmospheric pCO_2 level and one that assumes only enough H^+ are removed from the calcifying fluid to maintain a constant $[H^+]_E/[H^+]_I$ (i.e., variable H^+ -removal) under each atmospheric pCO_2 level. It should be noted that these two conditions were not selected for their mechanistic accuracy, but because they represent end-member scenarios for investigating the energetic requirements and carbonate system dynamics of calcification via H^+ -removal from the calcifying fluid.

Carbonate system parameters of the model were calculated for the site of calcification and for the external seawater with the program CO_2SYS (Lewis and Wallace, 1998) using Roy et al. (1993) values for the stoichiometric carbonic acid constants K^*_1 and K^*_2 , the Mucci (1983) value for the stoichiometric aragonite solubility product, $T = 25 \text{ °C}$, $S = 32$, $P = 1.015 \text{ atm}$, $TA = 2000\text{--}5545 \text{ } \mu\text{mol/kg-SW}$, $DIC = 1756, 1824, 1884, 2029 \text{ } \mu\text{mol/kg-SW}$, and $pCO_2 = 400, 600, 900, \text{ and } 2850 \text{ ppm}$ (see Table 1). Total alkalinity at the site of calcification was calculated as the external seawater alkalinity ($2000 \text{ } \mu\text{mol/kg-SW}$) plus the number of μmol of H^+ removed from 1 kg of the organism's calcifying fluid, as defined by Scenario 1 (fixed H^+ -removal) or Scenario 2 (fixed $[H^+]_E/[H^+]_I$)—since removing H^+ from the organism's calcifying fluid will, by definition, cause an equal-magnitude increase in its alkalinity. In the absence of DIC measurements of organisms' calcifying fluid, it is assumed in the model calculations to be equivalent to that of the external seawater. Nevertheless, in some organisms it is possible that additional DIC is respired and transported across cell membranes into the calcifying fluid or, alternatively, removed from the calcifying fluid of plants, algae

and/or organisms harboring photosynthesizing symbionts (e.g., zooxanthellate corals) via photosynthesis.

3.1. Scenario 1: Fixed H^+ -removal with variable $[H^+]_E/[H^+]_I$

Scenario 1 (Fig. 2A and Table 1) demonstrates how $[CO_3^{2-}]$ at the calcification site varies with atmospheric pCO_2 (400, 600, 900, 2850 ppm) for three hypothetical organisms that differ only in the number of H^+ that they are able to remove from a given volume of their calcifying fluid [external seawater (white diamonds); weak H^+ -pump (black circles) = $600 \text{ } \mu\text{mol } H^+/\text{kg-SW}$; moderate H^+ -pump (gray circles) = $2000 \text{ } \mu\text{mol } H^+/\text{kg-SW}$; and strong H^+ -pump (white circles) = $2900 \text{ } \mu\text{mol } H^+/\text{kg-SW}$]. Assuming that an organism removes a fixed number of H^+ from a given volume of its calcifying fluid under the four pCO_2 levels, $[H^+]_E/[H^+]_I$ (and therefore the energetic cost of removing each H^+) will increase with increasing atmospheric pCO_2 (Table 1).

3.2. Scenario 2: Fixed $[H^+]_E/[H^+]_I$ with variable H^+ -removal

Scenario 2 (Fig. 2B and Table 1) demonstrates how $[CO_3^{2-}]$ at the calcification site varies with atmospheric pCO_2 (400, 600, 900, 2850 ppm) for three hypothetical organisms that differ only in the H^+ -gradient ($[H^+]_E/[H^+]_I$) that they maintain across the membrane(s) that bounds their calcifying fluid [external seawater (white diamonds); weak $[H^+]_E/[H^+]_I$ (black circles) = 7:1; moderate $[H^+]_E/[H^+]_I$ (gray circles) = 45:1; strong $[H^+]_E/[H^+]_I$ (white circles) = 300:1]. Assuming that an organism maintains a fixed $[H^+]_E/[H^+]_I$, the number of H^+ removed from a given volume of its calcifying fluid (and therefore the energetic cost of removing H^+) will decrease with increasing atmospheric pCO_2 (Table 1).

3.3. Comparison of model scenarios

Both scenarios demonstrate that the response of calcification site $[CO_3^{2-}]$ to elevated pCO_2 becomes more negative as the strength of the H^+ -pump decreases (i.e., response is more negative for organisms that remove fewer H^+ from a given volume of calcifying fluid and/or maintain a lower $[H^+]_E/[H^+]_I$; Fig. 2 and Table 1). Both scenarios can also generate the full range of calcification response patterns observed in prior ocean acidification experiments (Figs. 1 and 2; e.g., Fabry et al., 2008; Doney et al., 2009; Ries et al., 2009). However, the energetic requirements of the two model scenarios are different. Scenario 1 (Fig. 2A) defines three hypothetical organisms that differ only in the number of H^+ that they remove from their calcifying fluid. The energetic requirements of H^+ -removal will increase with atmospheric pCO_2 for a given type of organism (i.e., weak, moderate, or strong H^+ -pump) because the given organism's $[H^+]_E/[H^+]_I$ will increase with atmospheric pCO_2 (Table 1), even though a fixed quantity of H^+ is removed. For example, the $[H^+]_E/[H^+]_I$ for an organism with a "moderate" H^+ -pump ($2000 \text{ } \mu\text{mol } H^+/\text{kg-SW}$) is approximately 140% greater at a pCO_2 of 2850 ppm than at a pCO_2 of 400 ppm (Table 1).

Table 1
Carbonate system constraints and energetic requirements of the two end-member calcifying fluid models.

	$p\text{CO}_2^{\text{a}}$	$[\text{H}^+]\text{-removed}^{\text{b}}$	$[\text{H}^+]_{\text{E}}/[\text{H}^+]_{\text{I}}^{\text{d}}$	$\Delta\text{-Energy}^{\text{e}}$ (%)	TA ^f	DIC ^g	pH	$[\text{HCO}_3^-]^{\text{h}}$	$[\text{CO}_3^{2-}]^{\text{i}}$	$\Omega_{\text{A}}^{\text{j}}$
<i>Fixed H^+-pump</i>										
External SW ^c	400	—	—	—	2000	1756	8.14	1570	175	2.8
	600	—	—	—	2000	1824	7.99	1674	133	2.1
	900	—	—	—	2000	1884	7.84	1760	98	1.6
	2850	—	—	—	2000	2029	7.37	1911	36	0.6
Weak H^+ -pump	400	600	4.8	0	2600	1756	8.82	1142	613	9.9
	600	600	5.7	18	2600	1824	8.75	1256	566	9.1
	900	600	7.0	45	2600	1884	8.68	1356	525	8.5
	2850	600	13.9	188	2600	2029	8.52	1601	423	6.8
Moderate H^+ -pump	400	2000	62	0	4000	1756	9.93	222	1534	24.8
	600	2000	69	12	4000	1824	9.83	281	1543	24.9
	900	2000	81	31	4000	1884	9.75	343	1541	24.9
	2850	2000	148	140	4000	2029	9.54	530	1499	24.2
Strong H^+ -pump	400	2900	191	0	4900	1756	10.42	79	1678	27.1
	600	2900	239	25	4900	1824	10.37	91	1733	28.0
	900	2900	304	59	4900	1884	10.32	105	1779	28.7
	2850	2900	643	236	4900	2029	10.18	153	1876	30.3
<i>Fixed $[\text{H}^+]_{\text{E}}/[\text{H}^+]_{\text{I}}$</i>										
External SW ^c	400	—	—	—	2000	1756	8.14	1570	175	2.8
	600	—	—	—	2000	1824	7.99	1674	133	2.1
	900	—	—	—	2000	1884	7.84	1760	98	1.6
	2850	—	—	—	2000	2029	7.37	1911	36	0.6
Weak $[\text{H}^+]_{\text{E}}/[\text{H}^+]_{\text{I}}$	400	805	7	0	2804	1756	8.99	986	770	12.4
	600	709	7	-12	2709	1824	8.84	1173	650	10.5
	900	601	7	-25	2602	1884	8.68	1355	526	8.5
	2850	348	7	-57	2348	2029	8.22	1781	237	3.8
Moderate $[\text{H}^+]_{\text{E}}/[\text{H}^+]_{\text{I}}$	400	1825	45	0	3825	1756	9.79	292	1464	23.6
	600	1768	45	-3	3768	1824	9.65	400	1424	23.0
	900	1678	45	-8	3678	1884	9.49	539	1345	21.7
	2850	1256	45	-31	3256	2029	9.03	1093	936	15.1
Strong $[\text{H}^+]_{\text{E}}/[\text{H}^+]_{\text{I}}$	400	3545	300	0	5545	1756	10.62	51	1705	27.5
	600	3163	300	-11	5163	1824	10.47	74	1751	28.3
	900	2883	300	-19	4883	1884	10.32	107	1777	28.7
	2850	2400	300	-32	4400	2029	9.85	302	1727	27.9

^a " $p\text{CO}_2$ " = CO_2 partial pressure of air in equilibrium with external seawater (ppm)

^b " $[\text{H}^+]\text{-removed}$ " = $[\text{H}^+]\text{-removed}$ from calcifying fluid ($\mu\text{mol}/\text{kg}\text{-SW}$) by proton pump

^c " SW " = seawater

^d " $[\text{H}^+]_{\text{E}}/[\text{H}^+]_{\text{I}}$ " = ratio of external seawater $[\text{H}^+]$ to calcifying fluid $[\text{H}^+]$

^e " $\Delta\text{-Energy}$ " = change in energy required to maintain given level of proton regulation relative to 400 ppm $p\text{CO}_2$ scenario, assuming that energy required varies linearly with $[\text{H}^+]\text{-removed}$ or $[\text{H}^+]_{\text{E}}/[\text{H}^+]_{\text{I}}$

^f " TA " = total alkalinity of fluid ($\mu\text{mol}/\text{kg}\text{-SW}$), calculated as external seawater TA plus $[\text{H}^+]\text{-removed}$ from calcifying fluid (assuming that seawater is the ultimate source of calcifying fluid—see text for discussion)

^g " DIC " = dissolved inorganic carbon of fluid ($\mu\text{mol}/\text{kg}\text{-SW}$)—calcifying fluid DIC is treated as equivalent to seawater DIC (assuming that seawater is the ultimate source of calcifying fluid—see text for discussion)

^h " $[\text{HCO}_3^-]$ " = bicarbonate ion concentration of fluid ($\mu\text{mol}/\text{kg}\text{-SW}$)

ⁱ " $[\text{CO}_3^{2-}]$ " = carbonate ion concentration of fluid ($\mu\text{mol}/\text{kg}\text{-SW}$)

^j " Ω_{A} " = saturation state of fluid with respect to aragonite

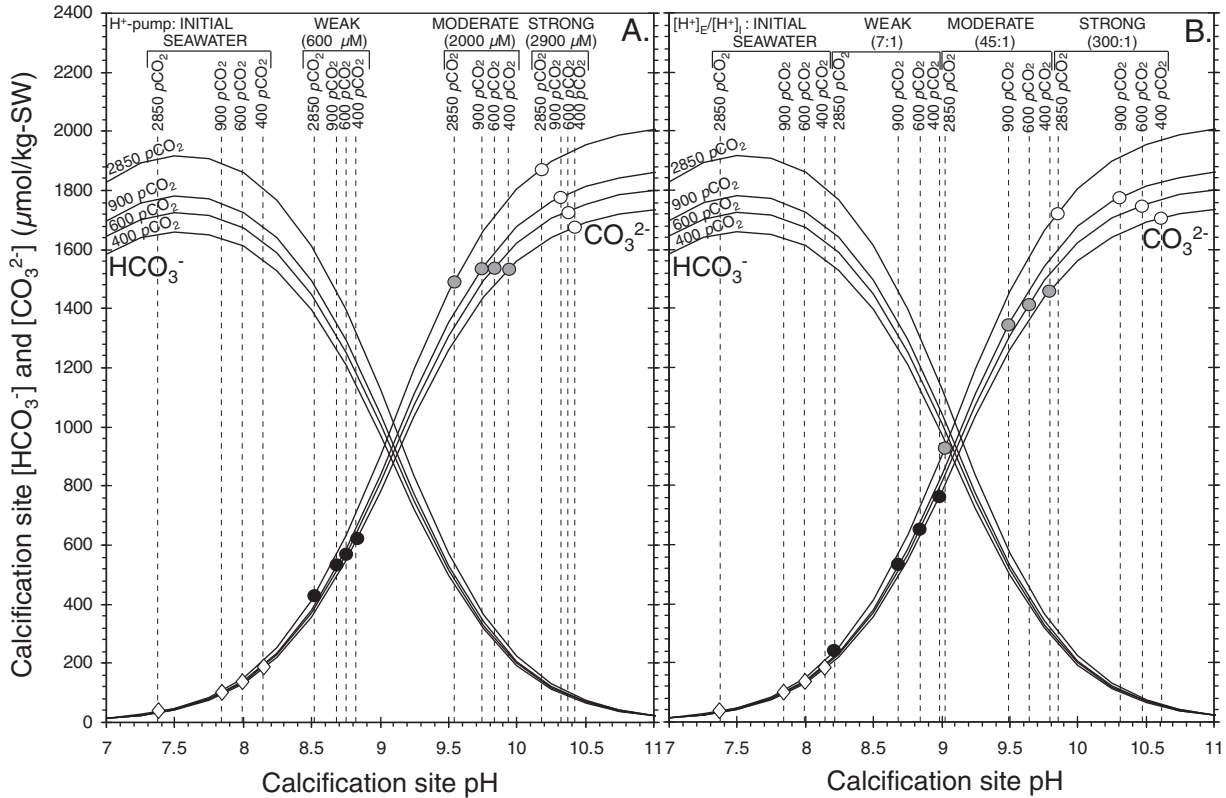


Fig. 2. Generalized proton-pumping model of marine organisms' calcifying fluids showing relationship between atmospheric $p\text{CO}_2$ (400, 600, 900, 2850 ppm), calcification site pH (x -axis), $[\text{CO}_3^{2-}]$ (circles), and $[\text{HCO}_3^-]$ for three hypothetical organisms differing only in the strength of their H^+ -regulating mechanism ("INITIAL SEAWATER" = white diamonds; "WEAK" = black circles, "MODERATE" = gray circles, "STRONG" = white circles; Table 1). (A) Scenario 1 assumes that an organism removes a fixed number of H^+ from a given volume of its calcifying fluid (variable $[\text{H}^+]_E/[\text{H}^+]_I$), regardless of atmospheric $p\text{CO}_2$ ("WEAK" H^+ -pump = $600 \mu\text{mol H}^+/\text{kg-SW}$; "MODERATE" H^+ -pump = $2000 \mu\text{mol H}^+/\text{kg-SW}$; "STRONG" H^+ -pump = $2900 \mu\text{mol H}^+/\text{kg-SW}$). (B) Scenario 2 assumes that an organism maintains a fixed $[\text{H}^+]_E/[\text{H}^+]_I$ (variable number of H^+ removed from a given volume of calcifying fluid) regardless of atmospheric $p\text{CO}_2$ ("WEAK" $[\text{H}^+]_E/[\text{H}^+]_I = 7:1$; "MODERATE" $[\text{H}^+]_E/[\text{H}^+]_I = 45:1$; "STRONG" $[\text{H}^+]_E/[\text{H}^+]_I = 300:1$). Both model scenarios are able to predict the full range of calcification responses observed in prior ocean acidification experiments (Fig. 1) and demonstrate that the calcification response to CO_2 -induced ocean acidification should be more negative for organisms that exert weaker control over their calcifying fluid pH (Ries et al., 2009). Microelectrode measurements of the calcifying fluid pH of the temperate coral *Astrangia poculata* (Table 2) suggest that the physicochemical dynamics of its calcifying fluid are most consistent with the model scenario that assumes a fixed $[\text{H}^+]_E/[\text{H}^+]_I$ (B).

The increased energetic cost of pumping the same number of H^+ against a steeper H^+ -gradient could cause energy to be diverted from other critical life processes under elevated $p\text{CO}_2$, such as tissue growth and/or reproduction (e.g., Wood et al., 2008).

Conversely, the energetic cost of maintaining a fixed $[\text{H}^+]_E/[\text{H}^+]_I$ (Scenario 2; Fig. 2B) should decrease with increasing atmospheric $p\text{CO}_2$ because the organism (i.e., weak, moderate, or strong $[\text{H}^+]_E/[\text{H}^+]_I$) would be required to pump fewer H^+ from a given volume of calcifying fluid in order to maintain a fixed $[\text{H}^+]_E/[\text{H}^+]_I$ under increasing atmospheric $p\text{CO}_2$ (Table 1). For example, an organism that maintains a "moderate" $[\text{H}^+]_E/[\text{H}^+]_I$ (45:1) would be required to remove approximately 31% fewer H^+ at a $p\text{CO}_2$ of 2850 ppm than at a $p\text{CO}_2$ of 400 ppm (Table 1). It should be noted that for approximately equivalent ranges of calcification site pH (e.g., black circles in Scenarios 1 and 2); Fig. 2 the response of $[\text{CO}_3^{2-}]$ at the site of calcification to elevated $p\text{CO}_2$ is generally more negative for hypothetical organisms that maintain a fixed $[\text{H}^+]_E/[\text{H}^+]_I$ (Scenario

2) than for those that remove a fixed number of H^+ from a given volume of their calcifying fluid (Scenario 1). However, as described above, the energetic demands of removing a fixed number of H^+ from a given volume of calcifying fluid (Scenario 1) will increase with increasing atmospheric $p\text{CO}_2$, while the energetic demands of maintaining a fixed $[\text{H}^+]_E/[\text{H}^+]_I$ (Scenario 2) will decrease with increasing atmospheric $p\text{CO}_2$.

4. MODEL EXPLORATION WITH THE TEMPERATE CORAL *ASTRANGIA POCULATA*

The calcifying fluid pH of the temperate coral *A. poculata* was measured with H^+ -sensitive microelectrodes under control and acidified conditions to investigate the applicability of the proposed model scenarios to calcification site pH-regulation within a temperate scleractinian coral.

This section should be prefaced with a brief overview of the two general models of coral calcification: the physicochemical model and the biological model (which are by

no means mutually exclusive). The physicochemical model of coral calcification (e.g., Constantz, 1986) asserts that corals accrete their skeletons by elevating the Ω_A of a calcifying fluid that is initially similar in composition to that of their external seawater, potentially via Ca^{2+} -ATPase-driven exchange of Ca^{2+} and H^+ ions across the coral tissue (e.g., Cohen and McConnaughey, 2003 and references therein; Al-Horani et al., 2003; McConnaughey, 2003; Cohen and Holcomb, 2009). The assertion in this model that the calcifying fluid of corals is initially similar to that of their external seawater is supported by measurements of elemental ratios within coral skeletons that are consistent with a Rayleigh-type distillation of discrete batches of a seawater-type fluid (Gaetani and Cohen, 2006; Cohen and Gaetani, 2010) and by observations that a decrease in the molar Mg/Ca ratio of corals' external seawater from the modern value of 5.2 [favoring the abiotic precipitation of aragonite and high-Mg calcite (calcite molar Mg/Ca > 0.04)] to 1.5 [favoring the abiotic precipitation of low-Mg calcite (calcite molar Mg/Ca < 0.04)] causes corals to accrete a portion of their skeleton as low-Mg calcite rather than aragonite (Ries et al., 2006; Ries, 2010a). The assertion in this model that corals accrete their skeletons by elevating the Ω_A of their calcifying fluid is supported by measurements of isotopic ratios within coral skeletons that are consistent with a calcifying fluid characterized by a strong pH gradient (e.g., Adkins et al., 2003) and by measurements of elevated pH (via pH microelectrodes; Al-Horani et al., 2003) and Ω_A (inferred from aragonite crystal aspect ratio; Cohen and Holcomb, 2009; Holcomb et al., 2009) of the coral calcifying fluid.

The biological model of coral calcification (cf. Cuif and Dauphin, 2005) asserts that calciblastic cells and organic matrices exert strong control over the coral mineralization process. This model is supported by direct observations of the tissue-skeleton interface (e.g., Clode and Marshall, 2002; Cuif and Dauphin, 2005; Tambutté et al., 2007), by the existence of desmocytes in the calciblastic epithelium of corals (e.g., Goldberg, 2001), by differential rates of calcification across the coral skeleton (e.g., Houlbreque et al., 2009), and by compositional variations in the coral skeleton that appear to be independent of thermo-chemical changes in the coral's external seawater (Meibom et al., 2008).

Regardless of which model most accurately describes the mechanism(s) by which corals calcify, the coral's ability to control pH and, thus, the carbonate chemistry at the site of calcification should play an important role in determining its calcification response to CO_2 -induced ocean acidification.

4.1. Materials and methods

4.1.1. Preparation of experimental seawaters

Two 10-L batches of 0.2 μm -filtered seawater were obtained from Vineyard Sound, Massachusetts. One 10-L batch was reserved as the control and the other 10-L batch was acidified with 2700 μL of a 1 M HCl solution. The experimental seawaters were maintained at 25 ± 0.1 °C (partial-immersion mercury-glass thermometer) using a 50-watt electric heater, salinity was 32.0 ± 0.1 (Autosal conductivity meter), total alkalinity of the normal and acidified

seawaters was 2001 ± 5 and 1732 ± 5 $\mu\text{mol/kg-SW}$, respectively (Gran titration calibrated with certified reference material provided by Prof. Andrew Dickson of the Scripps Institute of Oceanography, La Jolla, USA), and seawater pH of the normal and acidified seawaters was 8.16 ± 0.01 and 7.47 ± 0.01 , respectively (*Orion* pH electrode/meter calibrated with certified NBS pH buffers of 4.00, 7.00, 10.00; see discussion below). Total DIC, $[\text{CO}_3^{2-}]$, $[\text{HCO}_3^-]$, dissolved CO_2 ($[\text{CO}_2]_{\text{aq}}$), Ω_A , and $p\text{CO}_2$ of the gas in equilibrium with the experimental seawaters were calculated for the control and acidified treatments (Table 2) from measured values of temperature, salinity, total alkalinity, and pH using the program CO_2SYS (Lewis and Wallace, 1998) with Roy et al. (1993) values for the stoichiometric carbonic acid constants K^*_1 and K^*_2 , the Mucci (1983) value for the stoichiometric aragonite solubility product, and pressure of 1.015 atm (Table 2).

Ideally, ocean acidification experiments should be performed by varying atmospheric $p\text{CO}_2$, rather than through acid addition. However, the microelectrode approach employed in the present study was not compatible with the bubbling of CO_2 -enriched gas or with the flux of seawater previously bubbled with CO_2 -enriched gas into the vessel containing the coral, as the resulting turbulence destabilized the microelectrode. Thus, acidification was achieved by adding small aliquots of HCl to the seawater. It should be noted that the addition of HCl to lower the pH of the experimental seawater will also lower its total alkalinity and DIC (as the seawater was open to the atmosphere; Table 2), whereas lowering its pH via CO_2 bubbling will raise its DIC and not alter its total alkalinity. Nevertheless, the carbonate system parameters calculated for the experimental seawaters account for the effects of acid addition instead of CO_2 bubbling, as they were based upon measured pH and total alkalinity, which would have both been affected by (thereby accounting for) the acid addition.

4.1.2. Construction of pH microelectrodes

One-mm-diameter silanized glass capillary tubes were heated with a heating coil and machine-pulled to produce a tip diameter of approximately 1 μm . The 1- μm tip was sealed with a 3-mm membrane column of Hydrogen Ionophore II—Cocktail A (*Sigma-Aldrich*). The ionophore membrane was then backfilled with a 20–30-mm column of 0.2- μm -filtered 1 M KCl solution. The 1 M KCl electrolyte was connected to the reference with a Ag/AgCl wire. The microelectrodes were then mounted onto a micromanipulator that enabled their precise manipulation in three dimensions. The microelectrodes were calibrated with NBS pH buffers of 6.00, 7.00, 8.00, 9.00, 10.00, and 11.00 before its deployment and immediately after its removal from the calcifying fluid.

The use of NBS buffers to calibrate an electrode used to measure the pH of seawater (or calcifying fluid) generates an unknown and systematic error arising from the difference in liquid junction potentials between the two media. Comparison of pH calculated from the measured total alkalinity and DIC of a seawater sample with its pH measured using the NBS-calibrated microelectrodes suggests that this error was less than approximately 0.05 pH units,

Table 2

Carbonate system parameters of seawater and the calcifying fluid of the coral *Astrangia poculata* determined via pH microelectrode.

		Sal ^c	<i>T</i> ^d	pH	TA ^e	DIC ^f	<i>p</i> CO ₂ ^g	[HCO ₃ ⁻] ^h	[CO ₃ ²⁻] ⁱ	[CO ₂] _{aq} ^j	Ω _A ^k	[H ⁺] ^l	[H ⁺]-removed ^m	[H ⁺] _E /[H ⁺] _I ⁿ	
<i>Non-acidified seawater (control)</i>															
Trial 1	SW ^a	32	25	8.16	2001	1745	375	1552	183	11	3.0	6.8 × 10 ⁻³	2253	90.9	
	CF ^b	32	25	10.12	4254	1745	375	149	1596	0	25.8	7.5 × 10 ⁻⁵			
Trial 2	SW	32	25	8.18	2001	1739	362	1542	187	10	3.0	6.7 × 10 ⁻³	2359	103.8	
	CF	32	25	10.19	4360	1739	362	128	1611	0	26.0	6.4 × 10 ⁻⁵			
Trial 3	SW	32	25	8.15	2001	1755	396	1567	177	11	2.9	7.2 × 10 ⁻³	2062	68.5	
	CF	32	25	9.98	4063	1755	396	201	1554	0	25.1	1.0 × 10 ⁻⁴			
AVG (±SD)	SW	32 ± 0	25 ± 0	8.16 ± 0.02	2001 ± 2	1747 ± 8	377 ± 17	1554 ± 13	182 ± 5	11 ± 1	2.9 ± 0.1	6.9(±0.3) × 10 ⁻³	2225 ± 150	87.7 ± 17.8	
	CF	32 ± 0	25 ± 0	10.10 ± 0.11	4226 ± 150	1747 ± 8	377 ± 17	160 ± 38	1587 ± 30	0 ± 0	25.6 ± 0.5	8.1(±2.1) × 10 ⁻³			
<i>Acidified seawater</i>															
Trial 1	SW	32	25	7.47	1732	1729	1943	1634	39	56	0.6	3.4 × 10 ⁻²	1603	90.4	
	CF	32	25	9.43	3335	1729	1943	547	1182	0	19.1	3.7 × 10 ⁻⁴			
Trial 2	SW	32	25	7.48	1732	1726	1902	1632	40	55	0.6	3.3 × 10 ⁻²	1619	92.0	
	CF	32	25	9.44	3351	1726	1902	532	1194	0	19.3	3.6 × 10 ⁻⁴			
Trial 3	SW	32	25	7.46	1732	1731	1979	1635	38	57	0.6	3.4 × 10 ⁻²	1487	74.0	
	CF	32	25	9.33	3219	1731	1979	632	1099	0	17.7	4.6 × 10 ⁻⁴			
AVG (±SD)	SW	32 ± 0	25 ± 0	7.47 ± 0.01	1732 ± 2	1729 ± 2	1941 ± 39	1634 ± 2	39 ± 1	56 ± 1	0.6 ± 0.0	3.4(±0.1) × 10 ⁻²	1570 ± 72	85.5 ± 9.9	
	CF	32 ± 0	25 ± 0	9.40 ± 0.06	3302 ± 72	1729 ± 2	1941 ± 39	570 ± 54	1158 ± 52	0 ± 0	18.7 ± 0.8	4.0(±0.6) × 10 ⁻⁴			

^{f-k}DIC, *p*CO₂, [HCO₃⁻], [CO₃²⁻], [CO₂]_{aq}, and Ω_A of SW were calculated from measured sal, *T*, pH, and TA; TA, [HCO₃⁻], [CO₃²⁻], [CO₂]_{aq}, and Ω_A of CF were calculated from pH of the CF measured via microelectrode and from measured sal and *T* and calculated DIC of the external SW, each assumed to be equivalent for the CF on the premise that SW is ultimate source of CF (see text for discussion)

^a "SW" = seawater

^b "CF" = calcifying fluid

^c "Sal" = salinity

^d "*T*" = temperature (°C)

^e "TA" = total alkalinity (μmol/kg-SW)

^f "DIC" = dissolved inorganic carbon (μmol/kg-SW).

^g "*p*CO₂" = partial pressure of CO₂ of air in equilibrium with fluid (ppm); *p*CO₂ of SW and CF are assumed to be equivalent on the premise that SW is the ultimate source of CF (see text for discussion)

^h "[HCO₃⁻]" = bicarbonate ion concentration of fluid (μmol/kg-SW)

ⁱ "[CO₃²⁻]" = carbonate ion concentration of fluid (μmol/kg-SW)

^j "[CO₂]_{aq}" = CO₂ concentration of fluid (μmol/kg-SW)

^k "Ω_A" = saturation state of fluid with respect to aragonite

^l "[H⁺]" = proton concentration of fluid (μmol/kg-SW)

^m "[H⁺]-removed" = [H⁺]-removed from calcifying fluid (μmol/kg-SW), calculated from difference between total alkalinity of SW and CF after H⁺-removal (assuming composition of CF before H⁺-removal is equivalent to that of external SW)

ⁿ "[H⁺]_E/[H⁺]_I" = ratio of external seawater [H⁺] to calcifying fluid [H⁺]

which is less than the standard deviation in calcifying fluid pH amongst the three trials for both the acidified and control treatments. Thus, the error arising from the use of NBS buffers should not materially affect the reported results nor the interpretation of these results.

4.1.3. Measurement of calcifying fluid pH

Six ca. 4 cm-diameter coral colonies of *A. poculata* were harvested from Great Harbor of Vineyard Sound, Massachusetts, and maintained in an aquarium filled with Vineyard Sound seawater (25 °C) for approximately 7 days. One colony was immersed in a polypropylene container filled with 500 mL of the control seawater and allowed to acclimate for 1 h. The container of seawater and the coral were placed beneath a dissecting stereomicroscope illuminated with a ring lamp. A micromanipulator was used to insert an empty microelectrode tube through the coral's epithelial tissue layers at locations where the tissue layers were stretched taught across adjacent septal ridges of the corallite (Fig. 3). Once the empty microelectrode tube had contacted the coral skeleton, it was completely withdrawn from the coral, leaving behind an approximately 2–4- μm wide hole through the coral's tissue layers. A calibrated H^+ -selective microelectrode of similar dimensions to the empty microelectrode tube was then slowly inserted with the micromanipulator back through this hole to the point of contact with the skeleton, and then moved away from

the skeleton by approximately 1–2 μm (Fig. 3; McConnaughey and Whelan, 1997; Al-Horani et al., 2003). Although the author is not aware of any direct measurement of the thickness of coral calcifying fluid, the observation that the aragonite needles that make up the coral skeleton are typically longer than 3 μm (e.g., Cohen and McConnaughey, 2003) suggests that the calcifying fluid is at least that thick. Thus, the positioning of the microelectrode tip within 1 μm of the coral skeleton surface, combined with the consistently elevated pH values that the microelectrode registered at this location, suggests that the tip of the microelectrode was indeed positioned within the coral's calcifying fluid.

Approximately 10 min after insertion of the microelectrode, the coral's epithelial tissue closed around the microelectrode, effectively sealing off its calcifying fluid from the external seawater. The microelectrodes were deployed until a minimum of 20 min of stable pH data were obtained (at 20-s intervals). Calcifying fluid pH (Table 2) was calculated from the microelectrode voltage over the measured interval, pursuant to the calibration of the microelectrode that was conducted immediately after its removal from the calcifying fluid. External seawater pH was also monitored at 20-s intervals throughout the experiment. This process was repeated for two additional coral colonies immersed in 500 mL aliquots of the control seawater and for three additional coral colonies immersed in 500 mL aliquots of the acidified seawater (Table 2).

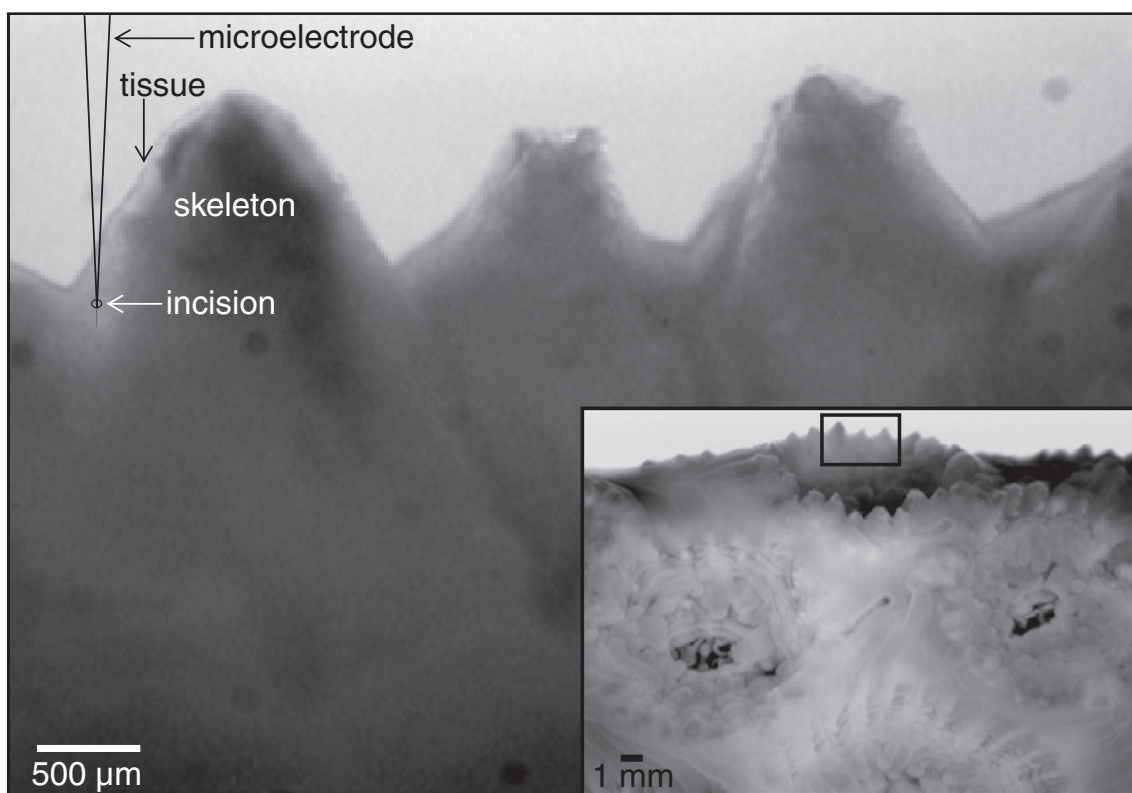


Fig. 3. Micrograph of the coral *Astrangia poculata* diagramming the approximate location where the pH microelectrode was inserted through the coral's epithelial tissues and into its putative calcifying fluid. Microelectrodes were inserted at the junction of adjacent septal ridges, where the coral's epithelial tissues were stretched most taughtly—rendering the calcifying fluid easier to access with the pH microelectrode. The higher magnification micrograph corresponds to the rectangle within the lower magnification image (inset).

4.1.4. Carbonate system calculations

Total alkalinity, $[\text{CO}_3^{2-}]$, $[\text{HCO}_3^-]$, dissolved CO_2 ($[\text{CO}_2]_{\text{aq}}$), and Ω_A of the corals' calcifying fluid under the control and acidified treatments (Table 2) were calculated using the program CO_2SYS (as described above) from the microelectrode pH measurements and from temperature, salinity, and DIC of the external seawater, which the model assumes are transferred to the coral's calcifying fluid (i.e., model assumes that seawater is the ultimate source of the calcifying fluid; e.g., Gaetani and Cohen, 2006). Again, it is possible that DIC is added to the calcifying fluid via respiration or, alternatively, removed via photosynthesis, causing calcifying fluid DIC to deviate from that of the external seawater—its putative source. Yet in the absence of direct measurements of calcifying fluid DIC, it is assumed to be equivalent to DIC of the external seawater. H^+ -removal was calculated as the difference between the measured total alkalinity of the external seawater (assumed to be the initial total alkalinity of the calcifying fluid) and the total alkalinity calculated for the calcifying fluid (Table 2).

4.2. Carbonate system chemistry of the calcifying fluid of *A. poculata*

The pH and Ω_A of the coral's calcifying fluid under the control treatment was 10.10 ± 0.11 and 25.6 ± 0.5 , elevated by approximately 1.9 and 23 units relative to external seawater pH (8.16 ± 0.02) and Ω_A (2.9 ± 0.1 ; Table 2). These measurements reveal that under non-acidified conditions, *A. poculata* promotes calcification by maintaining a substantially elevated pH and Ω_A within its calcifying fluid. These results are generally consistent with a set of microelectrode measurements that show that pH of the calcifying fluid of the tropical scleractinian coral *Galaxea fascicularis* is substantially elevated (up to pH 9.3) relative to the coral's external seawater pH of 8.2 (Al-Horani et al., 2003). These results are also generally consistent with previous studies that used the crystal aspect ratio of coral skeletal aragonite to deduce that the calcifying fluids of the temperate scleractinian coral *Astrangia poculata* (Cohen and Holcomb, 2009) and the tropical scleractinian corals *Diploria labyrinthiformis*, *Porites lutea*, *Porites solida* (Holcomb et al., 2009), and *Favia fragum* (Cohen and Holcomb, 2009) are substantially elevated relative to the corals' external seawater.

The microelectrode measurements revealed that *A. poculata* maintains its calcifying fluid at elevated pH (9.40 ± 0.06) and elevated Ω_A (18.7 ± 0.8) under acidified conditions, as well, although at lower values than those maintained under the control treatment. Although there are no published microelectrode measurements of calcifying fluid pH for corals reared under acidified conditions to which these observations can be compared, a decrease in the calcifying fluid Ω_A of *F. fragum* to approximately 2–3 in seawater acidified to a Ω_A of 0.6 has been inferred from the crystal aspect ratio of the coral's skeletal aragonite (Cohen and Holcomb, 2009). This is inconsistent with the observation that *A. poculata* is able to maintain a calcifying fluid Ω_A of approximately 19 as the Ω_A of its external seawater is reduced to 0.6. This discrepancy may reflect

species-specific differences between *A. poculata* and *F. fragum*, differences in the health and/or nutritional status of the coral specimens that were investigated, and/or differences in the developmental stages of the corals studied (e.g., *A. poculata* specimens were colonial adults while *F. fragum* specimens were solitary new-recruits).

4.3. *Astrangia poculata* maintains a fixed external-internal H^+ -ratio and removes fewer H^+ under elevated $p\text{CO}_2$

Critically, the $[\text{H}^+]_{\text{E}}/[\text{H}^+]_{\text{I}}$ maintained by *A. poculata* under the control treatment ($[\text{H}^+]_{\text{E}}/[\text{H}^+]_{\text{I}} = 88 \pm 18$) was not significantly ($p < 0.05$) different than that maintained under the acidified treatment ($[\text{H}^+]_{\text{E}}/[\text{H}^+]_{\text{I}} = 86 \pm 10$; Table 2). However, the corals removed significantly ($p < 0.05$) more H^+ from their calcifying fluid under the control treatment ($2225 \pm 150 \mu\text{mol H}^+/\text{kg-SW}$ removed) than under the acidified treatment ($1570 \pm 72 \mu\text{mol H}^+/\text{kg-SW}$ removed; Table 2). This observation is consistent with previous studies showing that the $[\text{H}^+]_{\text{E}}/[\text{H}^+]_{\text{I}}$ of marine algal cells remains nearly constant when seawater pH is reduced from 8 to 6 (Kitasato, 1968; Richards and Hope, 1974). This is surprising, nonetheless, because it reveals that *A. poculata* does not attempt to offset the reduction in seawater $[\text{CO}_3^{2-}]$ under acidified conditions by pumping more H^+ from its calcifying fluid. Instead, it appears to remove fewer H^+ from its calcifying fluid under acidified conditions, resulting in even lower $[\text{CO}_3^{2-}]$ at the site of calcification and, presumably, slower rates of calcification.

Although the end-member scenarios presented here were intended only to serve as a tool for exploring the proposed H^+ -pumping model of biological calcification under conditions of elevated $p\text{CO}_2$, the microelectrode measurements suggest that H^+ -regulation at the site of calcification of the temperate coral *A. poculata* is indeed consistent with the fixed $[\text{H}^+]_{\text{E}}/[\text{H}^+]_{\text{I}}$ scenario (Scenario 2). However, as is the case for most experimental perturbation studies, the corals were exposed relatively rapidly to the experimental conditions, and their responses measured over comparably short intervals of time (on the order of hours). Therefore, the measured changes in pH and, thus, carbonate chemistry at the site of calcification represent the corals' plastic (i.e., phenotypic) responses to CO_2 -induced ocean acidification, and provide little insight into their potential evolutionary (i.e., genotypic) responses. Furthermore, there was minimal water circulation in the incubation chambers, which may have influenced the corals' ability to exchange ions between their calcifying fluid and their external seawater. Thus, future experiments of this type would ideally be conducted over longer durations—potentially across multiple generations of organisms—under experimental conditions that more closely mimic natural conditions.

4.4. Implications for the response of *A. poculata* to ocean acidification

The microelectrode measurements suggest that Ω_A at the site of calcification of *A. poculata* will decrease from approximately 26 to 19 as external seawater is acidified from a pH of 8.16 to 7.47, which corresponds to an increase

in imputed $p\text{CO}_2$ from 377 to 1941 ppm. If a reduction in calcifying fluid Ω_A causes a reduction in the rate of coral calcification, then this suggests that calcification rates would decline for *A. poculata* as seawater acidifies due to rising atmospheric $p\text{CO}_2$. This prediction is consistent with experimental work (Holcomb et al., 2010) showing that calcification rates of *A. poculata* decline by more than 50% as atmospheric $p\text{CO}_2$ increases from 380 ($\Omega_A = 3.0$) to 760 ppm ($\Omega_A = 1.8$). Yet Holcomb et al. (2010) also showed that calcification rates of *A. poculata* are unimpaired by this increase in atmospheric $p\text{CO}_2$ when reared under nutrient-enriched conditions. It is possible that the increased nutrient levels promoted higher rates of photosynthesis by the corals' endosymbionts, which provided additional energy (as translocated photosynthate) for H^+ -regulation at the site of calcification (i.e., shifted the coral's response to the right in Fig. 2B), enabling it to maintain a higher $[\text{H}^+]_E/[\text{H}^+]_I$ and calcification site Ω_A under conditions of elevated nutrients (Holcomb et al., 2010). However, interpretation of Holcomb et al.'s (2010) results in the context of the present microelectrode experiment is limited by the fact that they investigated the calcification response of *A. poculata* to increased $p\text{CO}_2$ in seawater of similar alkalinities, while the present study investigated the coral's response to increased $p\text{CO}_2$ in seawater of decreased alkalinities.

5. APPLICABILITY OF THE PROPOSED MODEL TO UNDERSTANDING AND PREDICTING MARINE CALCIFIERS' RESPONSES TO CO_2 -INDUCED OCEAN ACIDIFICATION

The two model scenarios of calcifying fluid chemistry proposed here, which assume that marine calcifiers induce calcification either by removing a fixed number of H^+ from their calcifying fluid (i.e., variable $[\text{H}^+]_E/[\text{H}^+]_I$; Scenario 1) or by maintaining a fixed $[\text{H}^+]_E/[\text{H}^+]_I$ (i.e., variable H^+ -removal; Scenario 2), represent only end-member scenarios of a theoretical physicochemical framework for interpreting the response of marine calcifiers to CO_2 -induced ocean acidification. They are not intended, in isolation, to describe or predict the response of any individual species. Nor should the ability of Scenario 1 and 2 to predict the disparate calcification responses observed in prior ocean acidification experiments (e.g., Fabry et al., 2008; Doney et al., 2009; Ries et al., 2009; Fig. 1) necessarily be interpreted as evidence of the model's mechanistic accuracy. Additional microelectrode investigations of the calcifying fluids of a range of marine calcifiers are required to rigorously evaluate the viability of the model and its various iterations.

It should also be noted that there is considerable variability amongst calcifying taxa, as well as uncertainty amongst workers in the field of biomineralization, as to the nature of the medium from which marine calcifiers produce their shells and skeletons. Corals are thought to accrete CaCO_3 directly from a discrete calcifying fluid (e.g., Cohen and McConnaughey, 2003 and references therein; Al-Horani et al., 2003; Gaetani and Cohen, 2006; Cohen and Holcomb, 2009), with mineralization sites and crystal orientations being influenced by organic templates and/or calciblastic cells (e.g., Goldberg, 2001; Cuif and Dauphin,

2005; Tambutté et al., 2007; Meibom et al., 2008). It has also been argued that mollusks secrete their shells from a discrete calcifying fluid known as the pallial fluid (e.g., Crenshaw, 1972), although hemocytes have also been implicated in molluscan shell formation (Mount et al., 2004). Calcifying bryopsidalean algae, such as halimeda (Borowitzka and Larkum, 1976; De Beer and Larkum, 2001; Ries, 2009), are also thought to precipitate their aragonite needles from a discrete calcifying fluid—with little or no biological control over crystal orientation. Likewise, crustacea are thought to nucleate their shells from a discrete calcifying fluid (Cameron, 1985)—a process that must occur rapidly within these molting organisms. Although the general distribution of mineralized structures within crustacea appears to be guided by organic templates, the fine-scale crystal organization within these structures is highly complex and does not appear to be governed by the gross morphology of the organic templates (Roer and Dillaman, 1984). Echinoids, in contrast, are thought to initiate calcification on Ca^{2+} -binding organic matrices within cellular vacuoles (Ameys et al., 1998).

Regardless of the exact composition (e.g., seawater vs. modified seawater) or nature (e.g., fluid vs. gel) of their calcifying media, or the mechanisms by which they accrete their CaCO_3 (e.g., organic templates vs. cellular mediation vs. proton-pumps vs. Ca^{2+} -ATPase), organisms' ability to control the pH of their calcifying media should strongly influence their ability to convert DIC into CO_3^{2-} , thereby impacting their specific calcification response to CO_2 -induced ocean acidification.

A potential weakness of the proton-pumping model is that the relative changes in $[\text{CO}_3^{2-}]$ at the site of calcification predicted in response to elevated $p\text{CO}_2$ (Fig. 2) are in some cases substantially less than the relative changes in net calcification rates observed in prior ocean acidification experiments (e.g., Ries et al., 2009; Fig. 1). These discrepancies may be partly attributable to a non-linear relationship between calcification site $[\text{CO}_3^{2-}]$ and net calcification rate—e.g., calcification may only commence once a threshold $[\text{CO}_3^{2-}]$ of the calcifying fluid is crossed. These discrepancies may also result from the existence of other factors influencing rates of biological calcification that are not incorporated in the proposed model, including the fertilization of photosynthesis under elevated $p\text{CO}_2$, which could provide additional energy for H^+ -regulation at the site of calcification, and/or dissolution of unprotected shell/skeleton in undersaturated conditions, which could convert a “positive” or “neutral” response in $[\text{CO}_3^{2-}]$ at the site of calcification (e.g., white circles in Fig. 2A and B) into a “parabolic” or “threshold-negative” response in net calcification (e.g., Fig. 1D and E). Elevated $[\text{H}^+]$ of seawater may also affect other aspects of organisms' physiology (e.g., Langdon et al., 2003; Michaelidis et al., 2005; Wood et al., 2008) that may impact calcification indirectly, yet which are not incorporated into the physicochemical model proposed here.

6. CONCLUSION

A physicochemical model of organisms' calcifying fluid is proposed and explored through two end-member scenarios:

one that assumes organisms remove a fixed number of H^+ from a given volume of their calcifying fluid (variable $[H^+]_E/[H^+]_I$) regardless of atmospheric pCO_2 , and another that assumes that organisms maintain a fixed $[H^+]_E/[H^+]_I$ (variable H^+ -removal). Both model scenarios are able to generate the full range of calcification responses observed in prior ocean acidification experiments and are consistent with the assertion that the calcification response to CO_2 -induced ocean acidification will be more negative for marine calcifiers that exert weaker control over the pH of their calcifying fluid (Ries et al., 2009). Microelectrode measurements reveal that pH (and therefore Ω_A) of the calcifying fluid of the temperate coral *A. poculata* is substantially elevated relative to external seawater pH under both control and acidified conditions, which is consistent with the principal assumption of the generalized H^+ -pumping model of calcification. The microelectrode measurements also revealed that *A. poculata* maintained the same $[H^+]_E/[H^+]_I$ under the control and acidified treatments, yet removed fewer H^+ from a given volume of its calcifying fluid under the acidified treatment. These results suggest that the fixed $[H^+]_E/[H^+]_I$ scenario is most applicable to this particular coral species. These models and measurements are among the first attempts to explore physicochemical changes in the calcifying fluids of marine calcifiers in response to CO_2 -induced ocean acidification. Future experiments performed on a range of marine calcifiers that simultaneously monitor the impact of CO_2 -induced ocean acidification on the composition of their calcifying fluids and on their net rates of calcification are required to evaluate and further constrain the theoretical framework presented here.

ACKNOWLEDGMENTS

The author acknowledges P. Smith and D. Borgdorff for assistance with the microelectrode measurements, and A. Cohen, D. McCorkle, M. Holcomb, J. Erez, A. Szmant, R. Whitehead, A. Taylor, and D. Allemand for their stimulating feedback on the ideas presented herein. The author also acknowledges three anonymous referees and A.E. Mucci, whose reviews improved the quality of this manuscript. This research was supported by a WHOI Ocean and Climate Change Postdoctoral Fellowship, NSF award #1031995, and a UNC faculty development grant.

REFERENCES

- Adkins J. F., Boyle E. A., Curry W. B. and Lutringer A. (2003) Stable isotopes in deep-sea corals and a new mechanism for 'vital effects'. *Geochim. Cosmochim. Acta* **67**, 1129–1143.
- Al-Horani F. A., Al-Moghrabi S. M. and DeBeer D. (2003) The mechanism of calcification and its relation to photosynthesis and respiration in the scleractinian coral *Galaxea fuscicularis*. *Mar. Biol.* **142**, 419–426.
- Ameye L., Compere P., Dille J. and Dubois P. (1998) Ultrastructure and cytochemistry of the early calcification site and of its mineralization organic matrix in *Paracentrotus lividus* (Echinodermata: Echinoidea). *Histochem. Cell. Biol.* **110**, 285–294.
- Borowitzka M. A. (1987) Calcification in algae—mechanisms and the role of metabolism. *Crit. Rev. Plant Sci.* **6**, 1–45.
- Borowitzka M. A. and Larkum A. W. D. (1976) Calcification in the green alga *Halimeda*. III: The sources of inorganic carbon for photosynthesis and calcification and a model of the mechanism of calcification. *J. Exp. Biol.* **27**, 879–893.
- Cameron J. N. (1985) Post-moult calcification in the blue crab (*Callinectes sapidus*): relationships between apparent net H^+ excretion, calcium and bicarbonate. *J. Exp. Biol.* **119**, 275–285.
- Clode P. L. and Marshall A. T. (2002) Low temperature FESEM of the calcifying interface of a scleractinian coral. *Tissue Cell* **34**, 187–198.
- Cohen A. L. and Gaetani G. A. (2010) Ion partitioning and the geochemistry of coral skeletons: solving the mystery of the vital effect. *EMU Notes Mineral.* **11**, 377–397.
- Cohen A. L. and Holcomb M. (2009) Why corals care about ocean acidification: uncovering the mechanism. *Oceanography* **22**, 118–127.
- Cohen A. L. and McConnaughey T. A. (2003) A geochemical perspective on coral mineralization. In *Biom mineralization* (eds. P. M. Dove, S. Weiner and J. J. De Yoreo), pp. 151–187. Reviews in Mineralogy and Geochemistry. The Mineralogical Society of America.
- Constantz B. R. (1986) Coral skeleton construction: a physicochemically dominated process. *Palaios* **1**, 152–157.
- Crenshaw M. A. (1972) The inorganic composition of molluscan extrapallial fluid. *Biol. Bull.* **143**, 506–512.
- Cuif J.-P. and Dauphin Y. (2005) The environmental recording unit in coral skeletons—a synthesis of structural and chemical evidences for a biochemically driven, stepping-growth process in fibres. *Biogeosciences* **2**, 61–73.
- De Beer D. and Larkum A. W. D. (2001) Photosynthesis and calcification in the calcifying algae *Halimeda discoidea* studied with microsensors. *Plant Cell Environ.* **24**, 1209–1217.
- Doney S. C., Fabry V. J., Feely R. A. and Kleypas J. A. (2009) Ocean acidification: the other CO_2 problem. *Ann. Rev. Mar. Sci.* **1**, 169–192.
- Fabry V. J., Seibel B. A., Feely R. A. and Orr J. C. (2008) Impacts of ocean acidification on marine fauna and ecosystem processes. *ICES J. Mar. Sci.* **65**, 414–432.
- Gaetani G. A. and Cohen A. L. (2006) Element partitioning during precipitation of aragonite from seawater: a framework for understanding paleoproxies. *Geochim. Cosmochim. Acta* **70**, 4617–4634.
- Goldberg W. M. (2001) Desmocytes in the calciblastic epithelium of the stony coral *Mycetophyllia reesi* and their attachment to the skeleton. *Tissue Cell* **33**, 388–394.
- Goldman D. E. (1943) Potential, impedance, and rectification in membranes. *J. Gen. Physiol.* **27**, 37–60.
- Hodgkin A. L. and Katz B. (1949) The effect of sodium ions on the electrical activity of the giant axon of the squid. *J. Physiol.* **108**, 37–77.
- Holcomb M., Cohen A. L., Gabitov R. I. and Hutter J. L. (2009) Compositional and morphological features of aragonite precipitated experimentally from seawater and biogenically by corals. *Geochim. Cosmochim. Acta* **17**, 4166–4179.
- Holcomb M., McCorkle D. C. and Cohen A. L. (2010) Long-term effects of nutrient and CO_2 enrichment on the temperate coral *Astrangia poculata*. *J. Exp. Mar. Biol. Ecol.* **386**, 27–33.
- Houlbreque F., Meibom A., Cuif J.-P., Stolarski J., Marrocchi J., Ferrier-Page C., Domart-Coulon I. and Dunbar R. B. (2009) Strontium-86 labeling experiments show spatially heterogeneous skeletal formation in the scleractinian coral *Porites porites*. *Geophys. Res. Lett.* **36**, L04604. doi:10.1029/2008GL036782.
- Iglesias-Rodriguez M. D., Halloran P. R., Rickaby R. E. M., Hall I. R., Colmenero-Hidalgo E., Gittins J. R., Green D. R. H., Tyrrell T., Gibbs S. J., von Dassow P., Rehm E., Armbrust E. V. and Boessenkool K. P. (2008) Phytoplankton calcification in a high- CO_2 world. *Science* **320**, 336–340.
- Kitasato H. (1968) The influence of H^+ on the membrane potential and ion fluxes of *Nitella*. *J. Gen. Physiol.* **52**, 60–87.

- Kleypas J. A., Feely R. A., Fabry V. J., Langdon C., Sabine C. S. and Robbins L. L. (2006) Impacts of Ocean Acidification on Coral Reefs and Other Marine Calcifiers: A Guide for Future Research. Report of a workshop held 18–20 April 2005, St. Petersburg, FL, 88 p.
- Langdon C. (2000) Review of experimental evidence for effects of CO₂ on calcification of reef-builders. In *Proceedings of the 9th International Coral Reef Symposium*. pp. 1091–1098.
- Langdon C., Broecker W. S., Hammond D. E., Glenn E., Fitzsimmons K., Nelson S. G., Peng T. H., Hajdas I. and Bonani G. (2003) Effect of elevated CO₂ on the community metabolism of an experimental coral reef. *Global Biogeochem. Cycles* **17**, 1101–1114.
- Lewis E. and Wallace D. W. R. (1998) Program developed for CO₂ system calculations. ORNL/CDIAC-105. Carbon Dioxide Information Analysis Center, Oak Ridge National Laboratory, US Department of Energy, Oak Ridge, Tennessee.
- Meibom A., Cuif J.-P., Houlbreque F., Mostefaouia S., Dauphin Y., Meibom K. L. and Dunbar R. (2008) Chemical variations at ultra-structural lengthscales in coral skeleton. *Geochim. Cosmochim. Acta* **72**, 1555–1569.
- McConnaughey T. A. (2003) Sub-equilibrium oxygen-18 and carbon-13 levels in biological carbonates and kinetic models. *Coral Reefs* **22**, 316–327.
- McConnaughey T. A. and Falk R. H. (1991) Calcium-proton exchange during algal calcification. *Biol. Bull.* **180**, 185–195.
- McConnaughey T. A. and Whelan J. F. (1997) Calcification generates protons for nutrient and bicarbonate uptake. *Earth Sci. Rev.* **42**, 95–117.
- Michaelidis B., Ouzounis C., Palaras A. and Poertner H. O. (2005) Effects of long-term moderate hypercapnia on acid-base balance and growth rate in marine mussels *Mytilus galloprovincialis*. *Mar. Ecol. Prog. Ser.* **293**, 109–118.
- Mount A. S., Wheeler A. P., Paradkar R. P. and Snider D. (2004) Hemocyte-mediated shell mineralization in the Eastern Oyster. *Science* **304**, 297–300.
- Mucci A. (1983) The solubility of calcite and aragonite in seawater at various salinities, temperatures, and one atmosphere total pressure. *Am. J. Sci.* **283**, 780–799.
- Richards J. L. and Hope A. B. (1974) The role of protons in determining membrane electrical characteristics in *Chara corallina*. *J. Membr. Biol.* **16**, 121–144.
- Ries J. B. (2010a) Geological and experimental evidence for secular variation in seawater Mg/Ca (calcite–aragonite seas) and its effects on marine biological calcification. *Biogeosciences* **7**, 2795–2849.
- Ries J. B. (2010b) Shell-shocked: how different creatures deal with an acidifying ocean. *Earth* **55**, 46–53.
- Ries J. B. (2009) Effects of secular variation in seawater Mg/Ca ratio (calcite–aragonite seas) on CaCO₃ sediment production by the calcareous algae *Halimeda*, *Penicillus* and *Udotea*—evidence from recent experiments and the geological record. *Terra Nova* **21**, 323–339.
- Ries J. B., Cohen A. L. and McCorkle D. C. (2009) Marine calcifiers exhibit mixed responses to CO₂-induced ocean acidification. *Geology* **37**, 1131–1134.
- Ries J. B., Stanley S. M. and Hardie L. A. (2006) Scleractinian corals produce calcite, and grow more slowly, in artificial Cretaceous seawater. *Geology* **34**, 525–528.
- Rink S., Kuhl M., Bijma J. and Spero H. J. (1998) Microsensor studies of photosynthesis and respiration in the symbiotic foraminifer *Orbulina universa*. *Mar. Biol.* **131**, 583–595.
- Rodolfo-Metalpa R., Martin S., Ferrier-Pages C. and Gattuso J. P. (2010) Response of the temperate coral *Cladocora caespitosa* to mid-and long-term exposure to pCO₂ and temperature levels projected for the year 2100 AD. *Biogeosciences* **7**, 289–300.
- Roer R. and Dillaman R. (1984) The structure and calcification of the crustacean cuticle. *Integr. Comp. Biol.* **24**, 893–909.
- Roy R. N., Roy L. N., Vogel K. M., Porter-Moore C., Pearson T., Good C. E., Millero F. J. and Campbell D. M. (1993) The dissociation constants of carbonic acid in seawater at salinities 5 to 45 and temperatures 0 to 45 °C. *Mar. Chem.* **44**, 249–267.
- Saddler H. D. W. (1970) The membrane potential of *Acetabularia mediterranea*. *J. Gen. Physiol.* **55**, 802–821.
- Tambutté E., Allemand D., Zoccola D., Meibom A., Lotto S., Caminiti N. and Tambutté S. (2007) Observations of the tissue-skeleton interface in the scleractinian coral *Stylophora pistillata*. *Coral Reefs* **26**, 517–529.
- Wood H. L., Spicer J. I. and Widdicombe S. (2008) Ocean acidification may increase calcification rates, but at a cost. *Proc. R. Soc. B Biol. Sci.* **275**, 1767–1773.

Associate editor: Alfonso Mucci